An Ultrasonic Series Resonant Converter With Integrated *L-C-T*

Marthinus C. Smit, Jan A. Ferreira, *Member, IEEE*, Jacobus D. Van Wyk, *Fellow, IEEE*, and M. Ehsani, *Senior Member, IEEE*

***Abstract*—The concept of an integrated structure for the capacitor, inductor and transformer of the series resonant converter is presented. It is shown that the necessary capacitance can be achieved by using a bifilar primary and the leakage inductance of the transformer replaces the physical inductor. By integrating three components into one it would be possible to save space, mass, volume and cost.**

NOMENCLATURE

a	Width of U-core
b	Height of U-core
C	Discrete capacitance
C_{o-n}	Distributed capacitance
d	Separation of bifilar primary conductors
h	Height of toroidal core
$K_{as1-asn}$	Distributed magnetic coupling between first bifilar primary conductor and secondary winding
$K_{bs1-bsn}$	Distributed magnetic coupling between second bifilar primary conductor and secondary winding
$K_{pp1-ppn}$	Distributed magnetic coupling between first and second bifilar primary conductors
l_i	Diameter of primary of U-core structure
l_o	Diameter of secondary of U-core structure
L	Discrete series inductance
L_{a1-an}	Distributed series inductance of first bifilar primary conductor
L_{b1-bn}	Distributed series inductance of second bifilar primary conductor
L_{s1-sn}	Distributed series inductance of secondary
Lm	Magnetizing inductance
L_σ	Leakage inductance
L_1	Discrete inductance of primary of transformer
L_2	Discrete inductance of secondary of transformer
m	Width and height of secondary of toroidal structure
n	Number of elements in the transmission line model
N_p	Number of primary turns
r_i	Inner radius of toroidal core
r_o	Outer radius of toroidal core
R_{a1-an}	Distributed series resistance of first bifilar primary conductor
R_{b1-bn}	Distributed series resistance of second bifilar primary conductor
R_p	Discrete resistance representing capacitor losses
R_{p0-pn}	Distributed resistance representing capacitor losses
R_{s1-sn}	Distributed series resistance of secondary winding
R_1	Discrete series resistance of primary winding
R_2	Discrete series resistance of secondary winding
w	Width of bifilar primary conductors
ϵ_o	Permittivity of free space
ϵ_r	Relative permittivity
μ_o	Permeability of free space
μ_r	Relative permeability

Manuscript received May 2, 1990; revised July 14, 1994.

M. C. Smit, J. A. Ferreira, and J. D. Van Wyk are with the Research group: Electronic Power Control, Energy Laboratory, Rand Afrikaans University, Johannesburg 2000, South Africa.

M. Ehsani is with the Power Electronics Laboratory, Texas A&M University, College Station, TX 77843 USA.

IEEE Log Number 9407249.

I. INTRODUCTION

A constant demand exists for ever decreasing size in switch mode supplies. The first step has been the introduction of resonant mode converters [1]. Such converters typically consist of a resonant tank, a transformer and an input or output filter. The soft-switching characteristics of these converters allow an order of magnitude higher frequency, thus reducing the size of the reactive components. A further concept towards a smaller package is introduced, namely the electromagnetic integration of the resonant tank and, if possible, the transformer into a single component. That has the potential to not only save mass and volume, but also to eventually reduce manufacturing costs.

The particular converter to be investigated is the well known series resonant converter shown in Fig. 1. In this paper it will be shown that it is possible to integrate the series circuit consisting of the capacitor, inductor and transformer into a single structure.

II. THE INTEGRATED *L-C-T* TRANSMISSION LINE

The first step towards a practical integrated *L-C-T* is to recognise that a three conductor transmission line structure can behave as a series capacitor, inductor and transformer. In microstrip theory [2] it is a well known technique to create a capacitor by using short sections of transmission line of a very low characteristic impedance. In Fig. 2 conductor 1 and 2 are spaced with a very thin dielectric and form the series capacitor in the series resonant converter. In microstrip circuits

0885-8993/95$04.00

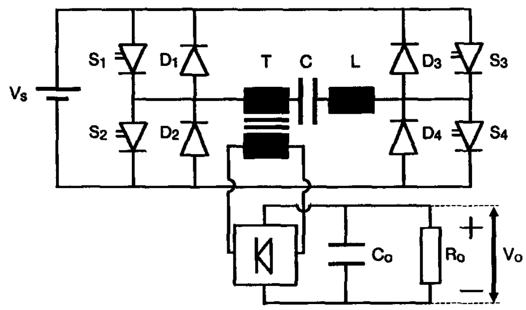

Fig. 1. The series resonant converter.

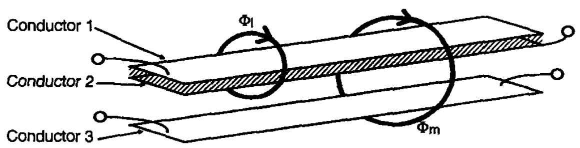

Fig. 2. The integrated *L-C-T* transmission line.

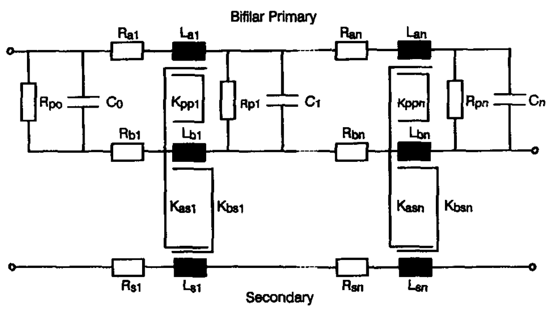

Fig. 3. Distributed circuit representation of the integrated *L-C-T* transmission line.

coupling between two circuits can be obtained by placing two conductor sections in close proximity to each other. In Fig. 2 conductor 3 has been placed so that a mutual flux Φ_m couples conductor 3 with conductor 1 and 2. Due to the space between them, a certain leakage flux Φ_l also exists. This leakage flux gives an uncoupled inductance which can serve as the series inductance L in Fig. 1.

This transmission line can be modelled as a distributed circuit network as indicated in Fig. 3. Magnetic coupling between conductor 1 an 3 is indicated by K_{as}, and that between conductor 2 and 3 by K_{bs}. This network is used to simulate the behaviour of the integrated *L-C-T*. The transmission line structure as configured in Fig. 2 is not practical for power transmission and the operating frequencies, if microstrip technology is to be used, is beyond the capability of power semiconductors with sufficient power processing capabilities. It is therefore necessary to investigate more practical lower frequency structures which can operate at frequencies below 10 MHz. It is however necessary that the new structure behaves in the same manner as the transmission line structure, because the experimental and theoretical work conducted within the scope of this project, indicated that the distributed network is a workable alternative to the lumped *L-C-T*.

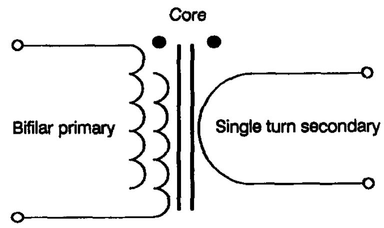

Fig. 4. Transformer diagram of the integrated *L-C-T*.

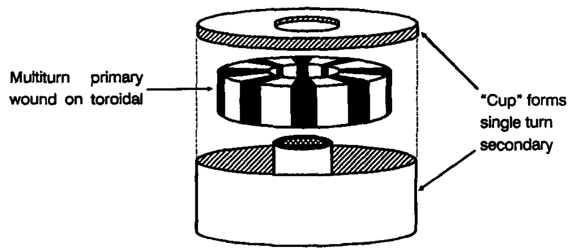

Fig. 5. Toroidal *L-C-T* transformer structure.

III. The Integrated *L-C-T* in a Transformer Structure

A suitable *L-C-T* structure for a series resonant converter requires a large enough LC product for a practical switching frequency, a suitable Z_0 to match the supply voltage and load and very good coupling between conductors 1, 2 and conductor 3 to facilitate power transmission. Good coupling can be achieved using a high frequency core, in which case the *L-C-T* structure becomes a transformer, as shown in Fig. 4. Conductors 1 and 2 in Fig. 2 have become a bifilar primary which contains the capacitor, while the leakage inductance serves as the series L (Fig. 1). Two structures were investigated experimentally.

The first involves a toroidal core as shown in Fig. 5. The primary consists of bifilar foil windings wound directly on the core [4]. The secondary has a single turn and forms a cup which contains the core and the primary. The space between the primary winding and the interior walls determine the leakage inductance.

Theoretical analysis of the toroidal structure is relatively easy due to the radial symmetry of the configuration. Manufacturing on the other hand is fairly complicated.

The second configuration is shown in Fig. 6 and consists of four U-cores positioned to form a cross, and I-core sections closing the magnetic circuit in the centre leg. Barrel type windings of foil conductors are used and construction is therefore easier than in the case of the toroidal structure. Theoretical analysis of this structure is more difficult, in particular calculation of leakage inductance. An approximation can be obtained by using the method outlined in reference [3].

IV. The Toroidal *L-C-T* Structure

The structure investigated in this section involves a transformer on a toroidal core, as is shown in Fig. 5. The specific design entails a single turn secondary and a multiturn primary. A toroidal configuration permits a very large range of leakage

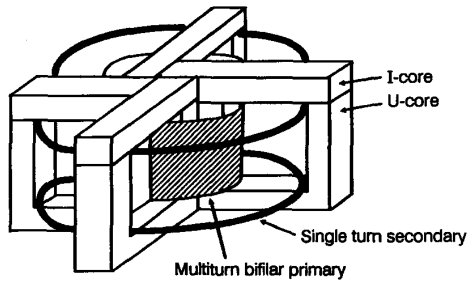

Fig. 6. U-core *L-C-T* transformer structure.

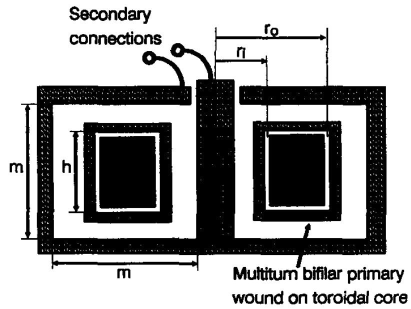

Fig. 7. Cross sectional dimensions of toroidal structure.

inductance values, since, contrary to other core configurations, the winding window is unbounded. For this configuration the theoretical analysis can then be performed with less approximation and verified with an experimental prototype.

A. Theoretical Analysis

Inductance: Calculation of the inductance of the structure is simplified by assuming that the magnetizing flux is confined to the volume of the core, and the leakage flux is confined to the volume enclosed between the multi turn bifilar primary and the single turn secondary winding. It can then be shown (Fig. 7) that the magnetizing inductance is given by:

$$L_m = \frac{\mu_0 \mu_r N_p^2 h(r_o - r_i)}{\pi(r_i + r_o)} \quad (1)$$

and the leakage inductance by:

$$L_\sigma = \frac{\mu_0 N_p^2 \left[m^2 - h(r_o - r_i)\right]}{\pi(r_i + r_o)} \quad (2)$$

where $N_p \equiv$ number of primary turns and m, h, r_i and r_o as defined in Fig. 7.

Capacitance: As can be seen from Figs. 2 and 4, the primary winding is constructed to form a capacitor by using a parallel strip bifilar wound winding, and bringing the opposite connections out. Assuming no fringe effects, the capacitance is given by:

$$C = \frac{2\varepsilon_0 \varepsilon_r N_p w(h + r_o - r_i)}{d} \quad (3)$$

where $d \equiv$ bifilar primary plate separation, $w \equiv$ bifilar primary plate width.

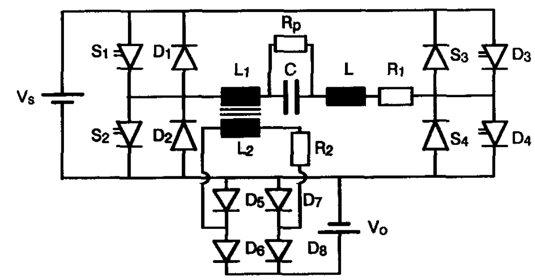

Fig. 8. SPICE model of discrete component converter.

B. Spice Simulation

The objective of the simulation is to show that the integrated structure reacts in the same way as a discrete series inductor capacitor and transformer would do, and in turn agrees with the experimental results. Fig. 8 shows the SPICE circuit model of the discrete component series resonant converter. Inductance L represents the leakage inductance of the structure, while the magnetizing inductance is represented by L_1. Since the secondary winding has only one turn, the inductance L_2 in the secondary of the converter is given by:

$$L_2 = \frac{L_1}{N_p^2} \quad (4)$$

Resistances R_1 and R_2 are the equivalent series (conduction) resistance of the converter primary and secondary respectively, and R_p models the capacive losses.

Fig. 9 shows the equivalent circuit representation of the integrated structure. The windings are modelled in terms of the transmission line in Fig. 3 and the component values are computed from the parameters used for discrete modelling (Fig. 8). It is assumed that no magnetic cross coupling exists and the coupling between conductors 1 and 2 (Fig. 2) is close to unity.

$$R_{a1} \cdots R_{an} = R_{b1} \cdots R_{bn} = \frac{R_1}{n} \quad (5)$$

$$L_{a1} \cdots L_{an} = L_{b1} \cdots L_{bn} = \frac{L_1}{n} \quad (6)$$

$$C_1 \cdots C_{n-1} = \frac{C}{n} \quad (7)$$

$$C_0; C_n = \frac{C}{2n} \quad (8)$$

$$R_{p1} \cdots R_{pn-1} = nR_p \quad (9)$$

$$R_{p0}; R_{pn} = 2nR_p \quad (10)$$

$$K_{pp1} \cdots K_{ppn} = 0.99999 \quad (11)$$

$$K_{as1} \cdots K_{asn} = K_{bs1} \cdots K_{bsn} = \sqrt{1 - \frac{L}{L_1}} \quad (12)$$

$$R_{s1} \cdots R_{sn} = \frac{R_2}{n} \quad (13)$$

$$L_{s1} \cdots L_{sn} = \frac{L_2}{n} \quad (14)$$

where n is the number of elements in the transmission line model.

These SPICE models are used to simulate both the frequency and time response described in the next paragraphs.

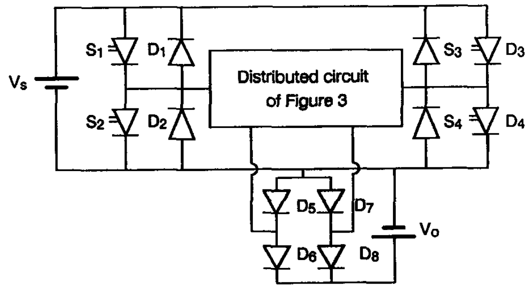

Fig. 9. SPICE model of integrated component converter.

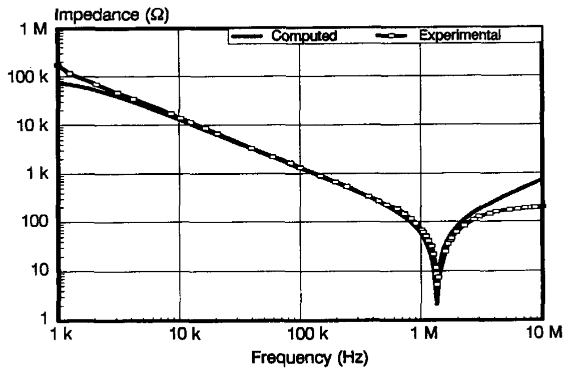

Fig. 10. Open circuit response.

Since it was shown [5] that little or no difference exists between the two SPICE models if the number of elements in Fig. 3 is greater than 10, the computed data of only one model is presented in each case.

C. Experimental Prototype

An experimental prototype was constructed, and had the following dimensions:

$$r_o = 18 \text{ mm} \quad r_i = 11.25 \text{ mm} \quad h = 15 \text{ mm}$$
$$\mu_r = 120 \quad \varepsilon_r = 2.67 \quad d = 25\,\mu\text{m}$$
$$N_p = 8 \text{ turns} \quad m = 20 \text{ mm} \quad w = 4 \text{ mm}$$

As shown in Figs. 10 and 11, an open circuit (secondary) resonant frequency (f_{open}) of 1.35 MHz was measured and a resonant frequency of 9 MHz was obtained when the secondary winding is shorted out (f_{short}).Transformer action of the integrated *L-C-T* is evident if the frequency response of the ratio, secondary output voltage to primary input voltage, is plotted. As shown in Fig. 12 the voltage ratio of 0.125 (eight turn primary and single turn secondary), is only evident at high frequencies where capacitance between the bifilar primary conductors is negligible. A comparison between the computed (Eqs. (1)–(3)) and experimental results are shown in Table I.

V. *U*-Core *LCT* Structure

The configuration is shown in Fig. 6 and is described in paragraph 3. The two winding bifilar primary (separated by a dielectric) and single turn secondary are wound through the

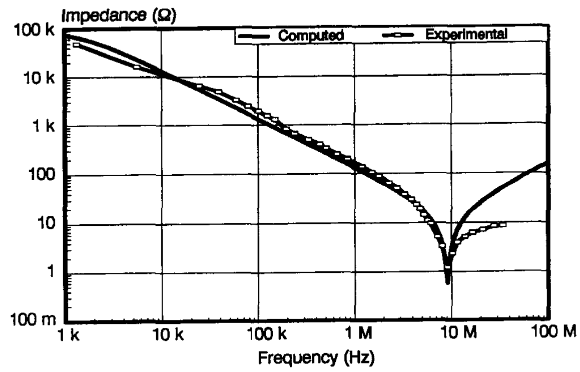

Fig. 11. Short circuit response.

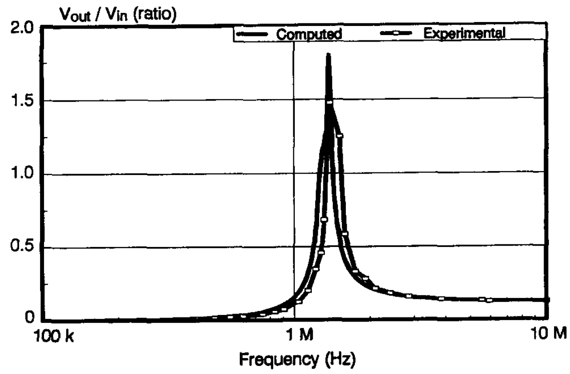

Fig. 12. V_{out} versus V_{in} ratio (secondary open circuit).

TABLE I
Difference Between Computed and Experimental Values (Toroidal Structure)

	L_m(μH)	L_σ(nH)	C(nF)	f_{open} (MHz)	f_{short} (MHz)
Computed	9.85	261.5	1.23	1.45	8.87
Experimental	11.56	255.4	1.2	1.35	9.1
Δ%	14.8	2.4	2.5	6.9	2.6

core window. Since in the present experimental configuration this structure is much larger than the toroidal structure, it results in a lower resonant frequency. (This configuration has been constructed in its present dimensions partly due to the available materials, and partly due to ease of experimental measurements).

A. Theoretical Analysis

Inductance: Using the same assumptions in calculating inductance in the U-core structure as for the toroidal structure, it can be shown (Fig. 13) that the magnetizing inductance is given by:

$$L_m = \frac{\mu_0 \mu_r N_p^2 l_i^2}{2(a+b)} \tag{15}$$

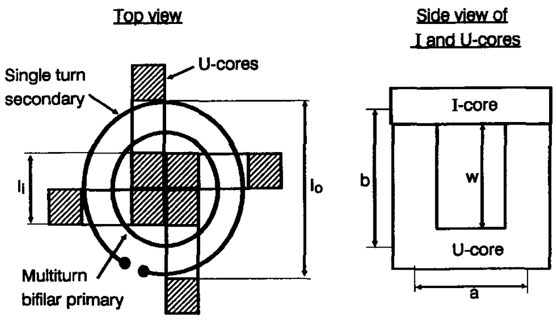

Fig. 13. Dimensions of *U*-core structure.

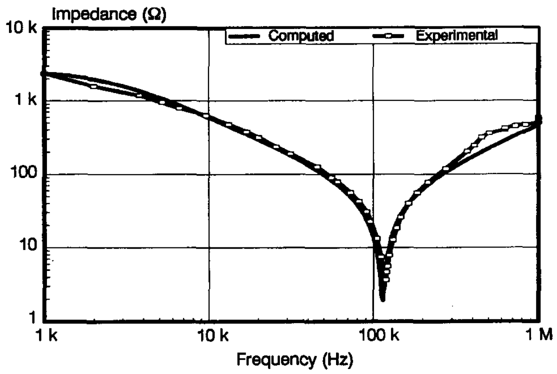

Fig. 14. Open circuit response.

and the leakage inductance by:

$$L_\sigma = \frac{\mu_0 N_p^2 \left[l_0^2 - l_i^2\right]}{w} \tag{16}$$

where $N_p \equiv$ number of primary turns, $w \equiv$ bifilar primary plate width.

Capacitance: Once again assuming no fringe effects, the capacitance is given by:

$$C = \frac{\sqrt{2}\pi\varepsilon_0\varepsilon_r N_p w l_i}{d} \tag{17}$$

where $d \equiv$ bifilar primary plate separation, $w \equiv$ bifilar primary plate width and l_i, l_o, a and b as defined in Fig. 13.

B. Experimental Prototype

The dimensions of an experimental prototype of the *U*-core structure are as follows:

$l_o = 135$ mm $l_i = 60$ mm $a = 70$ mm
$b = 70$ mm $w = 50$ mm $N_p = 2$ turns
$\mu_r = 1200$ $\varepsilon_r = 2.67$ $d = 25$ μm

C. Frequency Domain Performance

Using the capacitance of the bifilar primary (23.9 nF), the leakage and magnetizing inductance can be found by short- and open circuiting the secondary winding respectively. The open circuit resonant frequency was measured as 119 kHz,

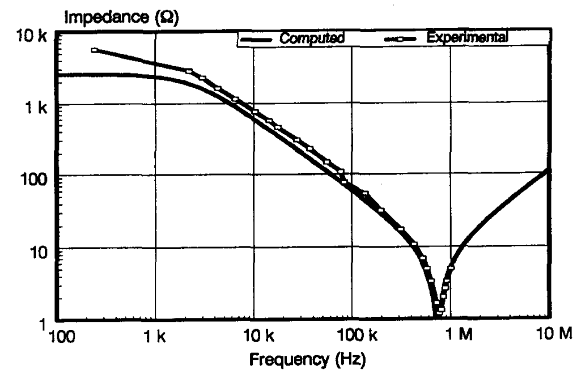

Fig. 15. Short circuit response.

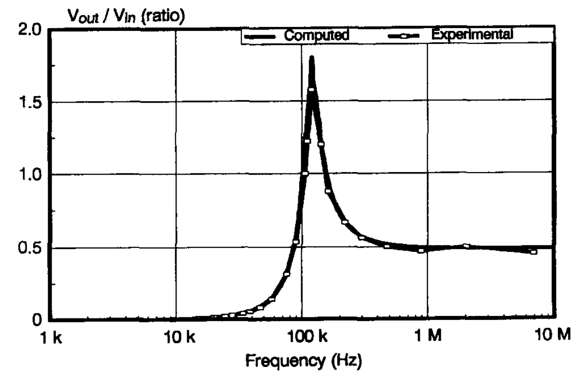

Fig. 16. V_{out} vs. V_{in} ratio (secondary open circuit).

TABLE II
DIFFERENCE BETWEEN COMPUTED AND EXPERIMENTAL VALUES (U-CORE STRUCTURE)

	$L_m(\mu H)$	$L\sigma(\mu H)$	C(nF)	f_{open} (kHz)	f_{short} (kHz)
Computer	77	1.47	22.5	120.9	875.1
Experimental	74.8	1.79	23.9	119	769.2
Δ%	2.9	17.9	5.6	1.6	12.1

which gives a magnetizing inductance of 75 μH. A resonant frequency of 769 kHz was obtained when the secondary winding shorted, corresponding to a leakage inductance of 1.8 μH (Figs. 14–16).

As suspected from the geometry of this structure and the assumptions made for the magnetic field distribution, the equation for the leakage inductance is not very accurate, but is adequate for an approximate analysis (Table II).

D. Time Domain

With a rectifier bridge, filter capacitor and 2.7 Ω load resistance, the applied voltage across and primary current of the *L-C-T* structure is shown in Fig. 17. From these time domain graphs it is evident that the integrated *L-C-T* structure functions well in a series resonant converter (Fig. 18). Agreement between experimental and simulated waveforms,

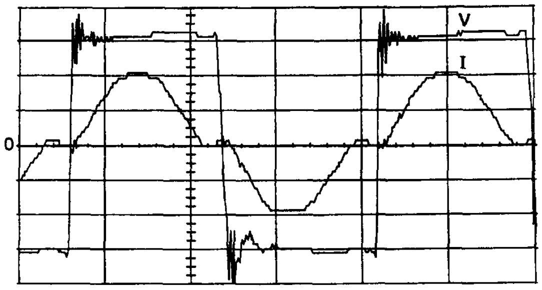

Vertical: 10 V/div. and 2 A/div.
Horizontal: 500 ns/div.

Fig. 17. Measured current and voltage waveforms of integrated component.

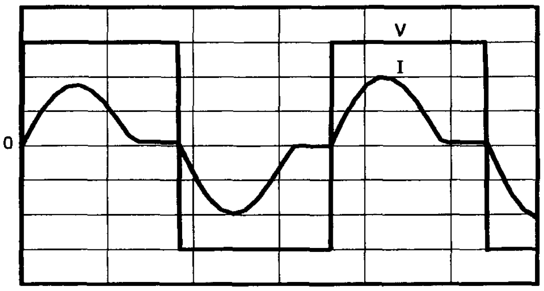

Vertical: 10 V/div. and 2 A/div.
Horizontal: 500 ns/div.

Fig. 18. Simulated current and voltage waveforms of integrated component converter.

as well as the similarity between the waveforms obtained with the lumped and distributed models [5], confirms the theoretical approach followed.

VI. Conclusion

A method to integrate the capacitor, inductor and transformer of a series resonant converter has been described. The results presented shows that an integrated L-C-T structure is practical and can successfully be modelled. The proposed component has been constructed and operated in a series resonant converter with success.

This integrated structure requires certain manufacturing technology which must be developed. A crucial technology is to be able to obtain large enough capacitance in the primary in order to get reasonable values of characteristic impedance and resonant frequency. This high permittivity would allow the integrated LCT-toroidal structure of this paper to be constructed with dimensions smaller than discrete components at an acceptable frequency, and would make this a competitive technology.

References

[1] F. C. Lee, "High frequency quasi-resonant converter technologies," *Proc. IEEE*, vol. 76, no. 4, 1988, pp. 377–390.

[2] T. C. Edwards, *Foundation for Microstrip Circuit Design,* John Wiley & Sons, 1981.

[3] P. L. Dowell, "Effects of Eddy currents in transformer winding," *Proceedings of the IEE*, vol. 113, no. 8, Aug. 1966, pp. 1387–1394.

[4] R. Reeves, "Inductor-capacitor hybrid," *Proc. IEE*, Nov. 1975, vol. 122, no. 11, pp. 1323–1326.

[5] M. C. Smit, "A new technology for integrated electromagnetic components for resonant power electronic converters," *M. Eng. Thesis*, Rand Afrikaans University, Dec. 1990.

Marthinus C. Smit was born in Johannesburg, South Africa, in 1967. He received the B.Eng. and M.Eng. degrees in electrical engineering from the Rand Afrikaans University, Johannesburg, South Africa, in 1989 and 1991, respectively.

His research interests lies in power electronics and electromagnetics, and he is currently employed by the CSIR, Pretoria, South Africa.

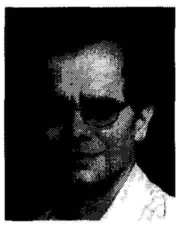

Jan A. Ferreira (M'88) was born in Pretoria, South Africa, in 1958. He received the B.Eng., M.Eng., and D.Eng. degrees in electrical engineering from the Rand Afrikaans University, Johannesburg, in 1980, 1982, and 1988, respectively.

In 1981, he worked at the Institute of Power Electronics and Electric Devices, Technical University of Aachen, and worked in industry from 1982–1985. Since 1986, he has been at the Faculty of Engineeering, Rand Afrikaans University, and currently holds the Carl and Emily Fuchs Chair of Power Electronics. He is author and coauthor of 50 papers and his research field includes magnetics, power electronics and manufacturing technology. Prof. Ferreira is current vice chairman of the IEEE South Africa section and chairman of the South African Energy chapter of the IEEE.

Jacobus D. van Wyk (F'90) was born in Fauresmith, South Africa in 1939. He received the M.Sc.Eng.-degree from the University of Pretoria, South Africa, and the Degree of Doctor of Technical Science, cum laude, from the University of Technology, Eindhoven, Netherlands, in 1966 and 1969, respectively.

He has worked with the S.A. Iron and Steel Corporation, the University of Pretoria, and was on the technical and scientific staff of the University in Eindhoven between 1961 and 1972. Since 1971 he has been a full Professor of Electrical and Electronic Engineering at the Rand Afrikaans University, Johannesburg, holding a chair in Power Electronics until 1992. He has been involved in extensive industrial work and is at present Programme Director of the Industrial Electronic Technology Research Group in the Faculty of Engineering as well as Vice-Rector of the University.

Since 1976 he has annually been appointed visiting professor in the Institute for Power Electronics and Electrical Drives of the University of Technology, Aachen, Germany. Since 1989 he is a member of the Graduate Faculty and Adjunct Professor at Texas Tech University, Lubbock, TX.

Dr. van Wyk is a Fellow of the IEEE, a Fellow of the South African Institute of Electrical Engineers, a Fellow of the S.A. Academy of Engineering, and a member of the Royal Dutch Institute of Engineers, and has been author or co-author of more than 200 publications. He has been co-recipient of seven IEEE prize paper awards for some of this work.

M. Ehsani (S'70–M'81-SM'83) received the B.S. and M.S. degrees from the University of Texas at Austin in 1973 and 1974, respectively, and the Ph.D. degree from the University of Wisconsin-Madison in 1981, all in electrical engineering.

From 1974 to 1977 he was with the Fusion Research Center, University of Texas, as a Research Engineer. From 1977 to 1981 he was with Argonne National Laboratory, Argonne, IL, as a Resident Research Associate, while simultaneously doing the doctoral work at the University of Wisconsin-Madision in energy systems and control systems. Since 1981 he has been at Texas A&M University, College Station, TX, where he is now Halliburton chaired Professor of electrical engineering and Director of Texas Applied Power Electronics Center (TAPC). He is the author of over 95 publications in pulsed-power supplies, high-voltage engineering, power electronics and motor drives, and is the recipient of the Prize Paper Award in Static Power Converters and motor drives at the IEEE-Industry Applications Society 1985, 1987, and 1992 Annual Meetings. In 1984 he was named the Outstanding Engineer of the Year by the Texas Society of Professional Engineers. He is also the co-author of a book on converter circuits for superconductive magnetic energy storage and a contributor to an IEEE Guide for Self-Commutated Converters and other monographs. He is the author of seven U.S. patents. His current research work is in power electronics, motor drives, hybrid vehicles and their control systems.

Dr. Ehsani is a member of the IEEE Power Electronics Society AdCom, Chairman of PELS Educational Affairs Committee, IEEE Industry Applications Society Executive Council, past Chairman of IEEE-IAS Industrial Power Converter Committee and chairman of the IEEE Myron Zucker Student-Faculty Grant program. He was the General Chair of the IEEE Power Electronics Specialists Conference for 1990 and was an IEEE Industrial Electronics Distinguished Speaker. He is also a registered professional engineer in the State of Texas.